Journal of Nuclear Medicine, published on December 1, 2016 as doi:10.2967/jnumed.116.179697

^{13}N-ammonia PET/CT detection of myocardial perfusion abnormalities in Beagle dogs after local heart irradiation

Jianbo Song[1,2], Rui Yan[1,3], Zhifang Wu[1], Jianguo Li[4], Min Yan[1], Xinzhong Hao[1], Jianzhong Liu[1], Sijin Li[1]

[1]Department of Nuclear Medicine, First Hospital of Shanxi Medical University, Shanxi, China;

[2]Department of Radiotherapy, Shanxi Academy of Medical Sciences, The Affiliated Shanxi Dayi Hospital of Shanxi Medical University, Shanxi, China;

[3]Nursing College, Shanxi Medical University, Shanxi, China;

[4]Department of Radiological and Environmental Medicine, China Institute for Radiation Protection, Shanxi, China.

First author: Jianbo Song, Department of Nuclear Medicine, First Hospital of Shanxi Medical University, No. 85, Jiefang Road, Taiyuan, Shanxi 030001, China.

Email: jianbo2611@126.com

Tel: (86)351-2170950

Corresponding author: Sijin Li(✉), MD, Department of Nuclear Medicine, First Hospital of Shanxi Medical University, No. 85, Jiefang Road, Taiyuan, Shanxi 030001, China.

Email: Lisj_nm1@sohu.com

Tel: (86) 351-4639278

Fax: (86)351-4048123

Word count: 4928

Financial disclosure: This study was supported by a grant from the Natural Science Foundation of China (No. 81171374).

Running title: ^{13}N-ammonia PET/CT MPI detection of RIHD

ABSTRACT

To determine the potential value of ^{13}N-ammonia positron emission tomography (PET)/computed tomography (CT) myocardial perfusion imaging (MPI) for detection of myocardial perfusion changes at early stage induced by radiation damage.

Methods: Thirty-six Beagle dogs were randomly divided into the control (n = 18) or the irradiation groups (n = 18). The irradiation group underwent local irradiation to the left ventricular anterior cardiac wall with a single dose of 20 Gy, whereas the control group received sham irradiation. All dogs underwent ^{13}N-ammonia PET/CT MPI one week before irradiation and at three, six, and twelve month after sham or local irradiation. One week after completing ^{13}N-ammonia PET/CT MPI examination, the irradiation group underwent coronary angiography examination. Six randomly selected Beagle dogs from each group were sacrificed and used to detect pathological cardiac injury at three, six, and twelve month after irradiation.

Results: Compared with the control group and baseline, the irradiation group showed significantly increased perfusion in the irradiated area of the heart at three month after irradiation, perfusion reduction at six month after irradiation, and perfusion defect at twelve month after irradiation. There was no significant difference in the left ventricular ejection fraction (LVEF) values between the control and irradiation groups at baseline and at three month after irradiation. The irradiation group showed a reduction of LVEF compared with the control group at six (50.0 ± 8.1% vs. 59.3 ±

4.1%, $p = 0.016$) and twelve month (47.2 ± 6.7% vs. 57.4 ± 3.3%, $p = 0.002$) after irradiation. No coronary stenosis was observed in the irradiation group. Regional wall motion abnormalities appeared in the irradiated area at six month after irradiation and its extent was enlarged at twelve month after irradiation. Pathological changes were observed, radiation-induced myocardial tissue damage and microvascular fibrosis was progressively increased with time prolonged in the irradiated area.

Conclusion: ^{13}N-ammonia PET/CT MPI can dynamically detect myocardial perfusion changes together with global and regional left ventricular dysfunction induced by irradiation and may be a valuable method for monitoring radiation-induced heart disease (RIHD).

Key words: Radiotherapy; radiation-induced heart disease; myocardial perfusion imaging; ^{13}N-ammonia PET/CT

INTRODUCTION

Radiotherapy is an effective treatment for many chest tumors, including breast cancer, lung cancer, esophageal cancer, Hodgkin's lymphoma, and so on. Several studies have demonstrated that radiation-induced heart disease (RIHD) increase in a dose-dependent manner in patients who undergo thoracic radiotherapy. Among these patients, RIHD is the most common non-cancer cause of death. The survival benefit obtained from radiotherapy can be counteracted by an increased risk of RIHD (*1-3*). Today, the heart is considered a key organ at risk from radiotherapy. With the development of sophisticated radiotherapy techniques, such as intensity-modulated radiation therapy, image-guided radiation therapy, and tomotherapy, radiation oncologists are able to deliver doses with far more accuracy than previous. This has resulted in a significant radiation dose reduction to cardiac tissue. However, most thoracic radiotherapy patients still receive either a high dose of radiation to a small part of the heart or a lower dose to the whole heart (*4-7*). It is important to note that there is no minimum threshold dose below which radiation is considered safe; even lower doses can increase the morbidity and the mortality of heart diseases (*8-11*). Because of the lack of convincing proof from multicenter trials with a sufficient follow-up period, the true incidence of RIHD is uncertain (*4,12*). Early diagnosis of RIHD can facilitate timely interventions and it may improve the prognosis of these patients. However, there are no currently accepted guidelines for RIHD screening and surveillance (*13-15*).

Therefore, the objective of this study was to investigate the perfusion changes with ^{13}N-ammonia PET/CT myocardial perfusion imaging (MPI) and the pathological changes in the same period in Beagle dog with RIHD models and to determine the feasibility of monitoring RIHD by ^{13}N-ammonia PET/CT MPI.

MATERIALS AND METHODS

Animals

In this study, all animals care and experimental procedures complied with the Institutional Animal Care and Use Committee Guidebook. Thirty-six Beagle dogs (all males, 12 month-old, weighing 12 ± 0.67 kg) were purchased from the Anhui Fuyang Weiguang Institute of Experimental Animals. After approximately 1 week of quarantine, the dogs were randomly assigned to the control group or the irradiation group which received local heart irradiation. All animals were housed individually in stainless steel cages in an air-conditioned facility(18 - 25 °C; relative humidity 40% - 60%; ≥ 12 air changes/h) and fed twice daily with standard certified commercial dog chow and water was available ad libitum at the Experimental Animal Center of the Chinese Academy of Radiation Medicine and Protection Institute. Before the study, the dogs were acclimated to these conditions for 2 weeks. All animals underwent ^{13}N-ammonia MPI, and

animals in the irradiation group underwent coronary angiography examination before irradiation and at three, six, and twelve month after local irradiation. Six animals randomly selected from each group were sacrificed at each time point, and their hearts were taken for pathological testing. The study was approved by our Institutional Animal Care and Use Committee and was performed in accordance with the Guidelines for Animal Experiments of Shanxi Medical University.

Local Heart Irradiation

Animals were anesthetized by intravenous injection with 3% pentobarbital sodium at 30 mg/kg and fixed by a vacuum-form body immobilizer in a supine position. All animals had a control-enhanced CT simulation scan (Discovery VCT64 PET/CT, General Electric, WI, USA) for radiotherapy planning. After scanning, the images were transmitted into the Varian eclipse TPS system. The anterior wall of the left ventricle was outlined as the radiation target, accounting for 1/4 - 1/3 of the left ventricular volume, and a conformal intensity-modulated radiation therapy plan was made. A cone beam CT was obtained with a flat-panel-detector to verify the accuracy of the target location prior to exposure. After location verification, the dogs in the irradiation group received a single dose of 20 Gy irradiation with 6 MV-X-ray, while the dogs in the control group received sham irradiation, simulating the same procedure but without irradiation.

^{13}N-ammonia MPI

After 12 hours of fasting, the dogs were anesthetized, attached to the vacuum-form body immobilizer in a supine position, transferred to the PET/CT (Discovery VCT, GE Healthcare, WI, USA) scanner bed, and connected to the electrocardiogram monitor. First, a CT scout was conducted to locate the position of the heart in the scanner field of view (FOV); the CT examination was performed with 120 kVp, 30 - 50 mA, and slice thickness of 3.75 mm. Next, 148 - 185 MBq (4 - 5 mCi) of ^{13}N-ammonia was administered by intravenous bolus injection. The PET scan was performed at three minutes after intravenous administration of the radiotracers. PET data were acquired in the 3D mode and lasted 10 minutes. Images were reconstructed using the iterative reconstruction method; the reconstruction matrix was 128 × 128 pixels, 2 iterations, and 6 subsets. Attenuation correction of PET images was performed by using attenuation data from the CT component of the examination.

Image Analysis

Images were processed using Myovation software in Xeleris 4.3(GE Healthcare) workstation. PET/CT images were independently reviewed by two experienced nuclear medicine physicians in a double-blind fashion; two observers analyzed all images in every subject slice-by-slice. In the semi-quantitative analysis, a same size region of interest (ROI) in both anterior wall (irradiated

area) and posterior wall (non-irradiated area) was delineated at three different levels of the ventricle on the PET/CT fusion images; the average radioactive counts was used for calculating the irradiation-to-non-irradiation (RAi/RAni) activity ratio. Gated studies were quantitatively analyzed by using the QGS software, the parameters of regional wall motion, end-diastolic volume (EDV), end-systolic volume (ESV), left ventricular ejection fraction (LVEF) were acquired automatically, and the polar bulls-eye plot was divided into 20 segments.

Coronary Angiography

One week after completing the ^{13}N-ammonia myocardial perfusion PET/CT examination, the irradiation group underwent coronary angiography examination. Anesthetized Beagle dogs were placed in the supine position after bilateral inguinal skin preparation. The multi-dimensional observation of the performance of coronary angiography was conducted in the catheterization laboratory by a cardiologist using a Judkin's catheter. Two experienced interventional cardiologists assessed the coronary angiography using the Thrombolysis in Myocardial Infarction score (*16*), which divides the coronary blood flow into four grades: 0 is no perfusion, 1 is penetration without perfusion, 2 is partial perfusion, and 3 is complete perfusion.

Histological Assessments

The Beagle dogs were euthanized under anesthesia by acute blood loss; the ribs were cut along the left sternal border, the thoracic cavity was exposed, and the heart was quickly removed. The atrial tissue was then removed from the heart, and the ventricular tissue was prepared for histological evaluation by immersion and fixation in 10% formalin. For each heart, myocardial tissue was taken from anterior wall (irradiated area) and posterior wall (non-irradiated area) respectively at the middle level of the left ventricle. All tissue samples were fixed and underwent tissue trimming, washing, and progressive dehydration in ethanol. The alcohol was then replaced with xylene, and the samples were embedded in a paraffin block. From each block, 5-μm-thick sections were prepared and stained with hematoxylin-eosin (HE), CD31 immunohistochemistry and Masson. Morphological changes were observed by light microscopy (JEM-2100; JEOL Company, Tokyo, Japan). Semi-quantitative measurement of myocardial degeneration and vascular injury was performed to evaluate the extent of cardiac damage (*17*,*18*).

For the evaluation of myocardial degeneration, six non-vascular microscopic fields (× 200) were randomly selected from the HE slices. The scoring criteria were as follows: 0 (normal): no degeneration of myocardial cells; 1 (mild): < 20% degeneration of myocardial cells; 2 (moderate): approximately 20% to 50% degeneration of myocardial cells; and 3 (severe): > 50% degeneration of myocardial cells.

For the evaluation of myocardial vascular injury, six vascular microscopic fields (× 200)

were randomly selected from the HE slices. The scoring criteria were: 0(normal): no fibrosis, adventitia thickness ≈ 1/2 media; 1(mild fibrosis): adventitia thickness ≈ media; 2 (moderate fibrosis): adventitia thickness ≈ 2x media; and 3 (severe fibrosis): adventitia thickness ≥ 3x media.

For the evaluation of myocardial microvessel density (MVD), six independent microscopic fields (× 200) were randomly selected from CD31 immunohistochemical staining slices. The percentage of blood vessels involved per visual field was graded as 0 (absent), 1 (< 10%), 2 (10-50%) and 3 (> 50%) (*19*).

For the evaluation of cardiac interstitial fibrosis, six independent microscopic fields (× 200) were randomly selected from Masson staining slices. The scoring criteria were: 0 (no apparent collagen fiber proliferation); 1 (focal and minimal fibrosis); 2 (mild patchy fibrosis); 3 (moderate diffuse fibrosis) and 4 (most prominent fibrosis) (*20*).

Statistical Analysis

All quantitative data were expressed as the means ± standard deviation. Differences between groups were tested using a t test and analysis of variance, and using rank sum test for ordinal data. Statistical significance was accepted at a level of $p < 0.05$. The SPSS 18.0 software package (SPSS Inc., Chicago, IL, USA) was used for statistical analyses.

RESULTS

Animal Conditions

One week before irradiation and at three, six, and twelve month after irradiation, the average weights of the animals in the irradiation group were 11.0 ± 1.0 kg, 13.0 ± 0.7 kg, 14.0 ± 1.0 kg, and 15.0 ± 0.7 kg, respectively. At the same time points, the average weights of the animals in the control group were 12.0 ± 0.1 kg, 13.0 ± 0.8 kg, 15.0 ± 0.1 kg and 15.0 ± 0.8 kg, respectively. There were no significant differences in the body conditions between the two groups in terms of diet, weight, heart rate, blood pressure, and mental status. No symptoms of heart failure were observed after irradiation.

^{13}N-ammonia PET/CT MPI

Compared to the control group and baseline, the irradiation group showed increased perfusion in the irradiated area of the heart at three month after irradiation; perfusion reduction were observed at six month after irradiation and perfusion defects at twelve month after irradiation (Figs. 1 and 2).

RAi/RAni Ratio

There were no significant differences in the RAi/RAni ratio between the control and irradiation groups before irradiation. Compared to the control group, RAi/RAni ratio in the irradiation group was increased at three month after irradiation (1.2 ± 0.1 vs. 1.0 ± 0.1, $p < 0.05$), decreased at six month (0.9 ± 0.3 vs. 1.0 ± 0.9, $p < 0.05$) after irradiation, and further significantly decreased at twelve month after irradiation (0.7 ± 0.4 vs. 1.0 ± 0.3, $p < 0.01$) (Table 1).

Parameters of Left Ventricular Function

No statistically significant differences were observed between the irradiation group and the control group in EDV, ESV, and LVEF before irradiation and at three month after irradiation. Similarly, there was no difference in EDV at six month after irradiation; however, ESV (13.4 ± 2.2 ml vs. 10.3 ± 1.7 ml, $p < 0.05$) was significantly higher and LVEF (50.0 ± 8.1 % vs. 59.3 ± 4.1%, $p < 0.05$) was significantly lower in the irradiation group compared with that in the control group. Interestingly, both EDV (26.5 ± 2.5 ml vs. 22.8 ± 3.2 ml, $p < 0.05$) and ESV (14.1 ± 2.0 ml vs. 10.4 ± 2.1 ml, $p < 0.01$) were significantly larger than that in control group, and LVEF (47.2 ± 6.7 % vs. 57.4 ± 3.3 %, $p < 0.01$) were significantly lower than that in control group at twelve month after irradiation (Table 2). No obvious abnormal ventricular wall motion was observed in two group animals at three month after irradiation. Regional ventricular wall-motion abnormalities were commonly observed in or adjacent irradiation area, and involved 5 segments at six month

after irradiation and involved 11 segments at twelve month after irradiation (Supplemental Table 1).

Coronary Angiography

No coronary stenosis was observed in the irradiation group at baseline, three, six, and twelve month after irradiation. All irradiation groups had Thrombolysis in Myocardial Infarction grade 3 coronary flow (Fig. 3).

Histological Results

In the control group, the myocardial tissue was normal, no significant changes were observed before and after irradiation (three, six, and twelve month) (Fig. 4A). Myocardial interstitial fibrosis was slightly increased in the irradiation area at three month after irradiation compared to the control group and non-irradiated area, and a small degree of fibrous tissue hyperplasia, interstitial small vessel wall thickening, and mild perivascular fibrosis was observed (Fig. 4B and Table 3). Six month after irradiation, some areas of the left ventricle showed myocardial degeneration, no myocardial necrosis, moderate myocardial interstitial fibrosis, and obvious interstitial small vessel wall thickening (Fig. 4C and Table 3). Twelve month after irradiation, the myocardial tissue had severe damage, a large degree of myocardial tissue degeneration and

myocardial interstitial fibrosis, significant interstitial vessel wall thickening, and severe perivascular fibrosis (Fig. 4D and Table 3). There was no obvious inflammatory cell infiltration in irradiation area. Masson staining showed that myocardial interstitial fibrosis was progressively increased after irradiation (Supplemental Fig. 1). Immunohistochemical staining show that myocardial interstitial MVD was significantly increased in the irradiation area at three month after irradiation revealed by CD31+ staining (Supplemental Fig. 2B). With the progression of radiation-induced myocardial tissue damage, myocardial interstitial MVD gradually decreased at six and twelve month after irradiation (Supplemental Fig. 2C and 2D). In the non-irradiated area, HE and Masson staining showed no significant abnormalities in myocardial tissue, and CD31 staining showed that a slight compensatory increase of MVD at three, six and twelve month after irradiation.

DISCUSSION

With the progress in radiotherapy technology, the disease-specific survival and the overall survival rates of cancer patients have been improved significantly. The issue of toxicity gradually gets more attention in thoracic radiation patients, and RIHD has been confirmed by animal experimental studies and clinical studies of cancer patients. Moreover, RIHD is often subclinical and may not manifest until years after radiotherapy, and its exact prevalence is unclear and, likely,

has been under-reported. The available evidence indicates that multidisciplinary follow-up and screening for RIHD is necessary (*13,14,21*). Early diagnosis of RIHD can promote timely clinical interventions and it may improve the prognosis of these patients, but the ideal screening method and frequency remain unclear, and the mechanisms of injury in RIHD remain largely unknown (*22*).

Marks et al. (*23,24*) conducted a prospective study to evaluate the changes in myocardial perfusion and cardiac function in irradiated patients for left-sided breast cancer, and 50% to 63% incidence of new perfusion defects was observed. Gayed et al. (*25,26*) reported a follow-up investigation with a small group of esophageal and lung cancer patients, who performed SPECT MPI after radiotherapy, and they found that myocardial perfusion abnormalities were often observed after radiotherapy. Furthermore, patients with perfusion defects are often clinically asymptomatic, and the long-term clinical significance of these perfusion abnormalities remains uncertain (*13,27,28*). In this study, we performed local irradiation to the anterior myocardial wall in Beagle dogs with a single 20Gy dose, which simulated a clinical high-dose radiation for local cardiac tissue and allowed comparison of the differences in the irradiated and non-irradiated areas, and at the same time period, we monitored the changes of myocardial blood flow in both the irradiated and non-irradiated areas by using ^{13}N-ammonia PET/CT MPI. In contrast to clinical investigation, animal experiments can eliminate the effects of irradiation position, dose/volume

differences, the inclusion criteria of chemotherapy, conventional high risks of heart disease, and other confounding factors.

In contrast to previous reports (*23-26*), we found that perfusion was increased in the irradiated field at three month after irradiation in the irradiation group compared with the non-irradiated tissue and the control group, and no functional changes were observed in the heart. These differences may have been due to scanning at different time points after radiation in different studies or because the ^{13}N-ammonia PET/CT MPI has higher sensitivity and specificity than SPECT MPI in precisely quantifying myocardial perfusion. The myocardial pathologic examination showed a small amount of myocardial cell degeneration, microvascular dilation, MVD increase and capillary wall thickening in the irradiated tissue; these injuries may have increased capillary permeability, resulting in increased perfusion flow. Six month after irradiation, in the irradiation group, the irradiated areas showed decreased perfusion, while cardiac function and LVEF was decreased. In clinical research, Gyenes et al (*29)* and Seddon B et al *(30*) also found that regional myocardial perfusion reduction was often observed in patients with left-sided breast cancer ≥ 6 months after radiotherapy. Pathology examination at the same time point identified mild myocardial degeneration, microvascular wall fibrosis and stenosis, and interstitial fibrosis. Twelve month after irradiation, the irradiated areas of the irradiation group animals exhibited myocardial perfusion defects, and left ventricular function was further reduced. In terms

of concomitant pathology, we found that radiation-related myocardial damage further aggravated, visible myocardial degeneration and a small area of myocardial necrosis, microvascular wall fibrosis, microvascular lumen stenosis and occlusion and interstitial fibrosis were significantly increased. RAi/RAni ratio, which could more accurately reflecting myocardial perfusion changes in the irradiation area than visual observation, and is less affected by the other factors, may be a more sensitive indicator for monitoring RIHD. Progressive increase of microvascular damage, myocardial degeneration and interstitial fibrosis may together result in the decrease of myocardial perfusion flow and regional left ventricular wall motion abnormalities at six and twelve month after irradiation. In general, myocardial fibrosis is a major endpoint for RIHD, microvascular damage and myocardial degeneration may aggravate myocardial fibrosis, and further work are warranted for further evaluating the exact biochemical mechanisms of RIHD.

From three to twelve months after irradiation, MPI perfusion abnormalities were spatially correlated to the 3D myocardial dose distribution computed with the CT dataset, while coronary angiography found no abnormalities. These results suggest that perfusion abnormalities caused by radiation-induced injury to the myocardial microvasculature are generally limited to the radiation field and do not correspond to the distribution of the coronary vessels.

CONCLUSION

^{13}N-ammonia PET/CT MPI can detect myocardial perfusion abnormalities together with global and regional left ventricular dysfunction induced by irradiation at very early stage of RIHD. Pathological examination and coronary angiography suggest that the early myocardial perfusion abnormalities induced by irradiation were due to microvascular damage, myocardial degeneration and interstitial fibrosis in the irradiated area, rather than by coronary artery stenosis. ^{13}N-ammonia PET/CT MPI may be a valuable method for monitoring and evaluating RIHD, though, its value in clinical practice will require further study for validation.

DISCLOSURE

This study was supported by a grant from the Natural Science Foundation of China (No. 81171374). The authors declared no conflicts of interest associated with this study.

ACKNOWLEDGMENTS

We would like to thank Dr. Xiaoli Zhang for help and advice of this manuscript. We give special thanks for the technical support we received from the Institute of Radiation Protection in China.

REFERENCES

1. Madan R, Benson R, Sharma DN, Julka PK, Rath GK. Radiation induced heart disease: pathogenesis, management and review literature. *J Egypt Natl Canc Inst.* 2015;27:187-193.

2. Chargari C, Riet F, Mazevet M, Morel E, Lepechoux C, Deutsch E. Complications of thoracic radiotherapy. *Presse Med.* 2013;42:e342-351.

3. Yan R, Song J, Wu Z, et al. Detection of myocardial metabolic abnormalities by 18F-FDG PET/CT and corresponding pathological changes in Beagles with local heart irradiation. *Korean J Radiol.* 2015;16:919-928.

4. Sridharan V, Tripathi P, Sharma S, et al. Roles of sensory nerves in the regulation of radiation-induced structural and functional changes in the heart. *Int J Radiat Oncol Biol Phys.* 2014;88:167-174.

5. Tillman GF, Pawlicki T, Koong AC, Goodman KA. Preoperative versus postoperative radiotherapy for locally advanced gastroesophageal junction and proximal gastric cancers: a comparison of normal tissue radiation doses. *Dis Esophagus.* 2008;21:437-444.

6. Weber DC, Peguret N, Dipasquale G, Cozzi L. Involved-node and involved-field volumetric modulated arc vs. fixed beam intensity-modulated radiotherapy for female patients with early-stage supra-diaphragmatic Hodgkin lymphoma: a comparative planning study. *Int J Radiat Oncol Biol Phys.* 2009;75:1578-1586.

7. Wu WC, Chan CL, Wong YW, Cuijpers JP. A study on the influence of breathing phases in intensity-modulated radiotherapy of lung tumours using four-dimensional CT. *Br J Radiol.* 2010;83:252-256.

8. Bhattacharya S, Asaithamby A. Ionizing radiation and heart risks. *Semin Cell Dev Biol.* 2016; 58:14-25.

9. Darby SC, Ewertz M, McGale P, et al. Risk of ischemic heart disease in women after radiotherapy for breast cancer. *N Engl J Med.* 2013;368:987-998.

10. Davis M, Witteles RM. Radiation-induced heart disease: an under-recognized entity? *Curr Treat Options Cardiovasc Med.* 2014;16:317.

11. Zagar TM, Marks LB. Breast cancer: risk of heart disease after radiotherapy-cause for concern. *Nat Rev Clin Oncol.* 2013;10:310-312.

12. Varga Z, Cserhati A, Rarosi F, et al. Individualized positioning for maximum heart protection during breast irradiation. *Acta Oncol.* 2014;53:58-64.

13. Groarke JD, Nguyen PL, Nohria A, Ferrari R, Cheng S, Moslehi J. Cardiovascular complications of radiation therapy for thoracic malignancies: the role for non-invasive imaging for detection of cardiovascular disease. *Eur Heart J.* 2014;35:612-623.

14. Lancellotti P, Nkomo VT, Badano LP, et al. Expert consensus for multi-modality imaging evaluation of cardiovascular complications of radiotherapy in adults: a report from the European Association of Cardiovascular Imaging and the American Society of Echocardiography. *Eur Heart J Cardiovasc Imaging.* 2013;14:721-740.

15. Chargari C. The issue of radiation-induced cardiovascular toxicity: preclinical highlights and perspectives on preventive strategies. *Biomed J.* 2013;36:150-151.

16. Narain VS, Fischer L, Puri A, Sethi R, Dwivedi SK. Prognostic value of angiographic perfusion score (APS) following percutaneous interventions in acute coronary syndromes. *Indian Heart J.* 2013;65:1-6.

17. Tokatli F, Uzal C, Doganay L, et al. The potential cardioprotective effects of amifostine in irradiated rats. *Int J Radiat Oncol Biol Phys.* 2004;58:1228-1234.

18. Dogan I, Sezen O, Sonmez B, et al. Myocardial perfusion alterations observed months after radiotherapy are related to the cellular damage. *Nuklearmedizin.* 2010;49:209-215.

19. Azimzadeh O, Sievert W, Sarioglu H, et al. PPAR alpha: a novel radiation target in locally exposed Mus musculus heart revealed by quantitative proteomics. *J Proteome Res.* 2013;12:2700-2714.

20. Singh VP, Le B, Khode R, Baker KM, Kumar R. Intracellular angiotensin II production in diabetic rats is correlated with cardiomyocyte apoptosis, oxidative stress, and cardiac fibrosis. *Diabetes.* 2008;57:3297-3306.

21. Martinou M, Gaya A. Cardiac complications after radical radiotherapy. *Semin Oncol.* 2013;40:178-185.

22. Stewart FA, Seemann I, Hoving S, Russell NS. Understanding radiation-induced cardiovascular damage and strategies for intervention. *Clin Oncol (R Coll Radiol).* 2013;25:617-624.

23. Marks LB, Yu X, Prosnitz RG, et al. The incidence and functional consequences of RT-associated cardiac perfusion defects. *Int J Radiat Oncol Biol Phys.* 2005;63:214-223.

24. Prosnitz RG, Marks LB. Radiation-induced heart disease: vigilance is still required. *J Clin Oncol.* 2005;23:7391-7394.

25. Gayed IW, Liu HH, Yusuf SW, et al. The prevalence of myocardial ischemia after concurrent chemoradiation therapy as detected by gated myocardial perfusion imaging in patients with esophageal cancer. *J Nucl Med.* 2006;47:1756-1762.

26. Gayed IW, Liu HH, Wei X, et al. Patterns of cardiac perfusion abnormalities after chemoradiotherapy in patients with lung cancer. *J Thorac Oncol.* 2009;4:179-184.

27. Yu X, Prosnitz RR, Zhou S, et al. Symptomatic cardiac events following radiation therapy for left-sided breast cancer: possible association with radiation therapy-induced changes in regional perfusion. *Clin Breast Cancer.* 2003;4:193-197.

28. Sioka C, Exarchopoulos T, Tasiou I, et al. Myocardial perfusion imaging with (99 m)Tc-tetrofosmin SPECT in breast cancer patients that received postoperative radiotherapy: a case-control study. *Radiat Oncol.* 2011;6:151.

29. Gyenes G, Fornander T, Carlens P, Glas U, Rutqvist LE. Detection of radiation-induced myocardial damage by technetium-99m sestamibi scintigraphy. *Eur J Nucl Med.* 1997;24:286-292.

30. Seddon B, Cook A, Gothard L, et al. Detection of defects in myocardial perfusion imaging in patients with early breast cancer treated with radiotherapy. *Radiother Oncol.* 2002;64:53-63.

Figure legends

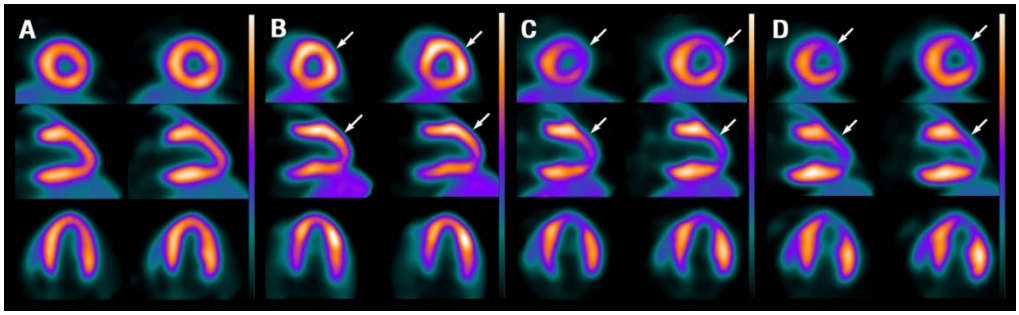

FIGURE 1. Irradiation group, ^{13}N-ammonia MPI at pre-radiation and three, six, and twelve month after irradiation. Normal myocardial perfusion before irradiation (A); increased perfusion at three month after irradiation (arrow, B); perfusion reduction at six month after irradiation (arrow, C); perfusion defect at twelve month after irradiation (arrow, D).

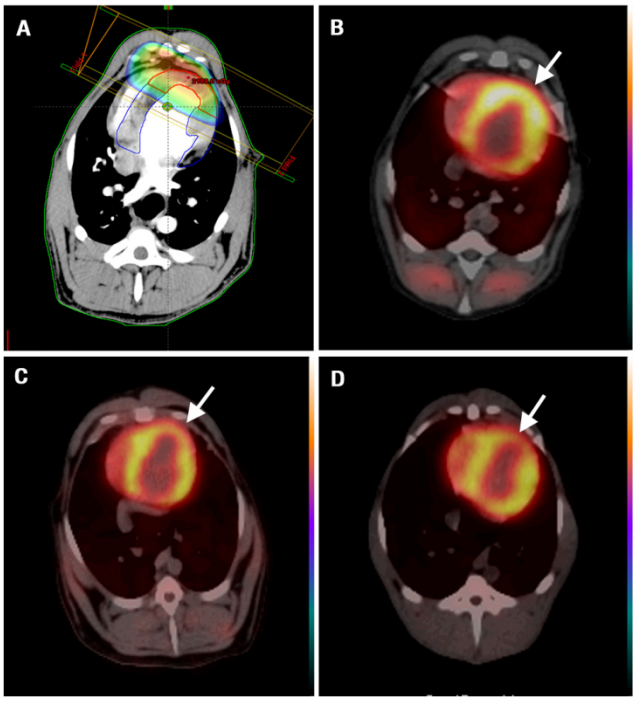

FIGURE 2. Radiation field and radiation dose distribution (A); PET/CT fusion images show that the scope of perfusion abnormality is consistent with the radiation field at three, six, and twelve month after irradiation (arrows, B-D).

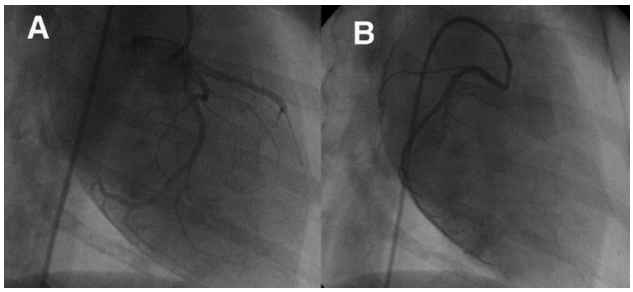

FIGURE 3. Coronary angiography in the irradiation group did not show coronary artery stenosis at twelve month after irradiation. Left coronary artery (A); right coronary artery (B).

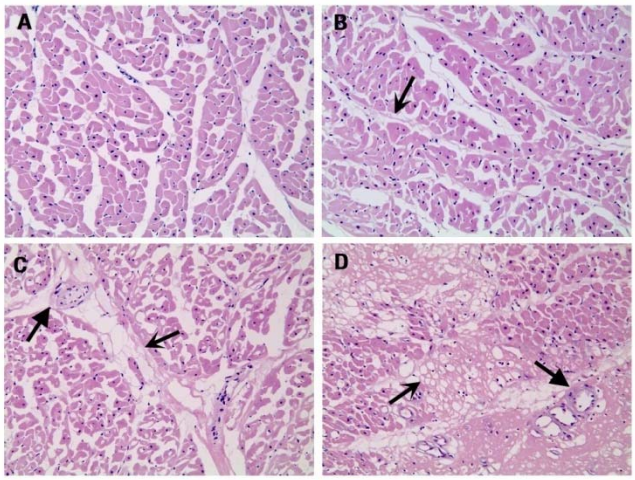

FIGURE 4. HE staining of myocardium in the control group (A) and irradiated myocardium in the irradiation group at three, six, and twelve month (B-D) at x200 magnification; (B) At three month after irradiation, mild myocardial cell deformation and interstitial fibers hyperplasia was observed (↑); (C) At six month after irradiation, obvious myocardial tissue degeneration, moderate myocardial interstitial fibrosis (↑)and vessel wall thickening was observed(↑); (D) At twelve month after irradiation, patchy myocardial necrosis and diffuse interstitial fibrosis(↑), significant vessel wall thickening and perivascular fibrosis was observed(↑).

TABLE 1

Comparison of the RAi/RAni ratio between the control and irradiation groups

Group	Prior to irradiation	Three month after irradiation	Six month after irradiation	Twelve month after irradiation
Control group	1.0 ± 0.1	1.0 ± 0.1	1.0 ± 0.9	1.0 ± 0.3
Irradiation group	1.1 ± 0.2	1.2 ± 0.1	0.9 ± 0.3	0.7 ± 0.4
p	0.9	0.047	0.015	< 0.01

TABLE 2

Comparison of functional parameters of left ventricle between the control and irradiation groups

Parameter	Prior to irradiation	Three month after irradiation	Six month after irradiation	Twelve month after irradiation
LVEF (%)				
Control Group	59.6 ± 5.2	58.9 ± 3.0	59.3 ± 4.1	57.4 ± 3.3
Irradiation Group	58.9 ± 5.6	56.4 ± 4.0	50.0 ± 8.1	47.2 ± 6.7
p	0.808	0.227	0.016	0.002
EDV(ml)				
Control Group	23.4 ± 2.8	23.4 ± 2.2	24.3 ± 2.3	22.8 ± 3.2
Irradiation Group	23.6 ± 2.6	23.9 ± 4.2	23.3 ± 3.6	26.5 ± 2.5
p	0.923	0.816	0.952	0.014
ESV(ml)				
Control Group	11.1 ± 2.1	11.2 ± 1. 5	10.3 ± 1.7	10.4 ± 2.1
Irradiation Group	10.4 ± 2.0	10.6 ± 4.7	13.4 ± 2.2	14.1 ± 2.0
p	0.490	0.491	0.01	0.001

LVEF = left ventricular ejection fraction; EDV = end-diastolic volume; ESV = end-systolic volume.

TABLE 3

Comparison of histological parameters between the control and irradiation groups

G	Myocardial degeneration						Myocardial vascular injury					
	3month		6month		12month		3month		6month		12month	
	C	I	C	I	C	I	C	I	C	I	C	I
0	30	6	31	4	28	2	31	10	32	2	29	0
1	4	25	3	10	6	3	2	19	1	11	5	5
2	1	3	2	16	1	11	2	4	2	18	2	14
3	1	2	0	6	1	20	1	3	1	5	0	16

G = grade; C = Control group; I = irradiation group.

Statistical analysis of data by rank sum test, compared with the control group, pathological changes in the irradiated area were significant, all *p* values are less than 0.05.

Supplemental Table 1

Segmental changes of WM in polar map

Segment	Pre-rad	3M post-rad	*p*	Pre-rad	6M post-rad	p	Pre-rad	12M post-rad	*p*
A									
basal	5.9 ± 0.3	5.6 ± 0.4	0.150	5.5 ± 0.4	5.1 ± 0.3	0.082	5.2 ± 0.3	4.7 ± 0.6	0.087
middle	5.5 ± 0.5	5.2 ± 0.7	0.474	5.3 ± 0.3	4.9 ± 0.4	0.082	5.3 ± 0.3	3.9 ± 0.8	0.003
apical	5.8 ± 0.4	5.3 ± 0.6	0.125	5.6 ± 0.5	4.1 ± 1.3	0.021	5.6 ± 0.5	4.4 ± 0.3	＜0.001
AS									
basal	3.4 ± 0.4	3.5 ± 0.9	0.640	3.4 ± 0.4	2.9 ± 0.1	0.013	3.4 ± 0.4	2.8 ± 0.4	0.029
middle	4.5 ± 0.7	4.6 ± 0.4	0.959	4.5 ± 0.7	4.7 ± 0.7	0.746	4.3 ± 0.4	3.5 ± 0.4	0.009
apical	5.6 ± 0.4	5.2 ± 0.6	0.207	5.3 ± 0.2	4.8 ± 0.6	0.115	5.3 ± 0.2	3.5 ± 1.1	0.002
IS									
basal	5.1 ± 0.3	5.0 ± 0.2	0.444	5.0 ± 0.2	4.0 ± 0.2	＜0.001	5.0 ± 0.2	4.2 ± 0.4	0.002
middle	5.9 ± 1.0	6.1 ± 0.4	0.630	5.4 ± 0.8	4.6 ± 0.6	0.065	5.3 ± 0.7	5.1 ± 0.5	0.695
apical	6.7 ± 0.3	6.4 ± 0.1	0.080	6.3 ± 0.2	6.4 ± 0.3	0.468	6.0 ± 0.1	5.5 ± 0.7	0.145
I									
basal	6.2 ± 0.5	6.3 ± 0.3	0.793	6.2 ± 0.5	6.1 ± 0.3	0.517	6.0 ± 0.3	5.9 ± 0.9	0.631
middle	6.4 ± 0.5	6.6 ± 0.2	0.504	6.3 ± 0.5	6.2 ± 0.3	0.550	6.1 ± 0.4	6.1 ± 0.1	0.663
apical	6.5 ± 0.3	6.5 ± 0.1	0.801	6.3 ± 0.1	6.3 ± 0.3	0.819	6.1 ± 0.2	5.9 ± 0.3	0.341
IL									
basal	6.4 ± 0.3	6.4 ± 0.2	1.000	6.2 ± 0.3	6.1 ± 0.6	0.900	6.0 ± 0.3	4.5 ± 0.4	0.000
middle	6.1 ± 0.3	6.3 ± 0.6	0.552	6.2 ± 0.2	6.1 ± 0.3	0.830	6.0 ± 0.2	6.1 ± 0.2	0.202
apical	6.4 ± 0.3	6.3 ± 0.3	0.641	6.2 ± 0.1	5.9 ± 1.0	0.488	5.9 ± 0.2	5.8 ± 0.3	0.276
AL									
basal	6.3 ± 0.3	6.4 ± 0.4	0.929	6.3 ± 0.3	5.2 ± 0.4	＜0.001	6.0 ± 0.2	4.8 ± 0.6	＜0.001
middle	6.0 ± 0.3	6.1 ± 0.4	0.777	6.0 ± 0.3	6.0 ± 0.6	0.951	5.8 ± 0.2	5.8 ± 0.5	0.888
apical	6.2 ± 0.5	6.5 ± 0.4	0.325	6.1 ± 0.4	6.3 ± 0.2	0.313	6.1 ± 0.4	3.9 ± 0.5	＜0.001
Apex									
A	6.1 ± 0.3	5.9 ± 0.6	0.499	6.1 ± 0.3	3.4 ± 1.4	0.001	6.1 ± 0.3	3.5 ± 0.6	＜0.001
I	6.1 ± 0.6	5.7 ± 0.3	0.151	5.9 ± 0.5	5.7 ± 1.2	0.703	6.0 ± 0.5	3.2 ± 0.4	＜0.001

WM = wall motion; Pre-rad = before irradiation; post-rad = Post-irradiation; M = mouth; A = anterior; AS = anteroseptal; IS = inferoseptal; I = inferior; IL =inferolateral; AL = anterolateral

Supplemental Figure 1

Masson staining

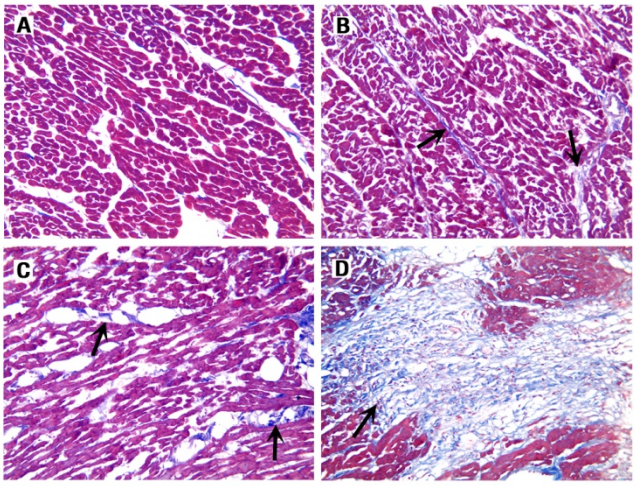

Supplemental Figure 1. Masson staining of myocardium in the control group (A) and in the irradiation group at 3, 6, and 12 month (B-D) after irradiation with x200 magnification; myocardial interstitial fibrosis was progressively increased with time prolonged after irradiation.

Supplemental Figure 2

CD31 immunohistochemical staining

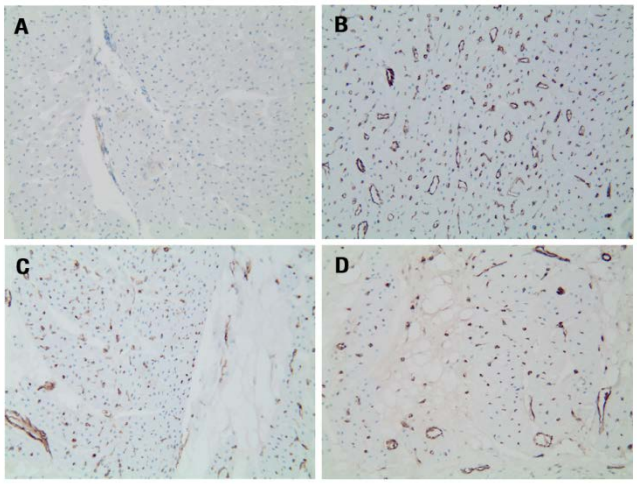

Supplemental Figure 2. CD31 immunohistochemical staining of myocardium in the control group (A) and in the irradiation group at 3, 6, and 12 month (B-D) with x200 magnification; Myocardial interstitial microvessel density was significantly increased in the irradiation area at three month after irradiation, and gradually decreased at six and twelve month after irradiation.